Marine Pollution Bulletin 187 (2023) 114491

Contents lists available at ScienceDirect

Marine Pollution Bulletin

journal homepage: www.elsevier.com/locate/marpolbul

Effects of estuarine water mixing on the mobility of trace elements in acid mine drainage leachates

Rafael Pérez-López [a,*], Ricardo Millán-Becerro [a], María Dolores Basallote [a], Sergio Carrero [b], Annika Parviainen [c,d], Rémi Freydier [e], Francisco Macías [a], Carlos R. Cánovas [a]

[a] Department of Earth Sciences & Research Center on Natural Resources, Health and the Environment, University of Huelva, Campus "El Carmen", E-21071 Huelva, Spain
[b] Institute of Environmental Assessment and Water Research (IDÆA-CSIC), E-08034 Barcelona, Spain
[c] Universidad de Granada, Departamento de Edafología y Química Agrícola, Avda. Fuente Nueva s/n, E-18071 Granada, Spain
[d] Instituto Andaluz de Ciencias de la Tierra (UGR-CSIC), Avda. de las Palmeras 4, E-18100 Armilla, Granada, Spain
[e] HSM, Université de Montpellier, CNRS, Montpellier, France

ARTICLE INFO

Keywords:
Mining pollution
Tinto and Odiel rivers
Estuary of Huelva
Seawater mixing
Contaminants mobility

ABSTRACT

This research reports the effects of pH increase on contaminant mobility in acid mine drainage from the Iberian Pyrite Belt by seawater mixing in the laboratory, simulating the processes occurring in the Estuary of Huelva (SW Iberian Peninsula). Concentrations of Al, Fe, As, Cu and REY in mixing solutions significantly decreased with increasing pH. Schwertmannite precipitation at pH 2.5–4.0 led to the total removal of Fe(III) and As. Subsequently, iron-depleted solutions began to be controlled by precipitation of basaluminite at pH 4.5–6.0, which acted as a sink for Al, Cu and REY. Nevertheless, as the pH rises, schwertmannite becomes unstable and releases back to solution the previously retained As. Moreover, other elements (S, Zn, Cd, Ni and Co) behaved conservatively in mixing solutions with no participation in precipitation processes. Some toxic elements finally end up to the Atlantic Ocean contributing to the total pollutant loads and environmentally threatening the coastal areas.

1. Introduction

Meteoric waters draining mining areas of sulfide-bearing ore deposits lead to the oxidation of sulfides and consequently generate acid mine drainage (AMD), which are leachates characterised by low pH values and high concentrations of sulfate, iron, aluminum, and potentially toxic elements such as As, Cu, Zn, Cd, Co and Ni, among others (Nordstrom, 2011). Human activities, especially related to abandoned mining facilities, cause environmental pollution due to the release of significant concentrations of these metal(loid)s into rivers that finally flow into the oceans.

Much research has focused on the behaviour of pollutants in AMD-affected fluvial courses. In watercourses, element concentrations can be affected by both precipitation of newly-formed phases and dilution by mixing with pristine receiving waters, resulting in a natural contamination attenuation downstream of point sources located in mining districts (Lambeth, 1999; Sarmiento et al., 2009). High concentrations of sulfate and ferric iron in AMD favour the spontaneous precipitation of schwertmannite ($Fe_8O_8(OH)_{(8-2x)}(SO_4)_x \cdot nH_2O$; with x varying from 1 to 1.75), a poorly crystalline and metastable oxyhydroxysulfate that commonly covers AMD-impacted riverbeds worldwide (Bigham et al., 1990, 1994; Yu et al., 1999; Fernandez-Martinez et al., 2010; Caraballo et al., 2013). Schwertmannite surface is protonated, and thus, is positively charged under acidic conditions, which favours the retention of oxyanions from solution, particularly As (Courtin-Nomade et al., 2003; Fukushi et al., 2003; Acero et al., 2006), but also Sb, Cr, Mo and V (Orden et al., 2021). Electrostatic repulsion between metal cations and the mineral surface, both positively charged, together with the acidity of solutions buffered by the release of protons involved in the schwertmannite precipitation, cause that the rest of the elements (e.g., Cd, Co, Ni, and Zn) mostly behave conservatively in streams at pH below 4.0; i.e., their concentrations only decrease by dilution but not by mineral precipitation (Braungardt et al., 2003).

Estuaries represent the transition zone between freshwater and seawater, regulating the flux of pollutants entering the coastal areas and ultimately the deep oceans. Geochemical processes controlling the mobility of contaminants in estuarine systems can be very complex and include a set of reactions transferring mass between dissolved and

* Corresponding author.
E-mail address: rafael.perez@dgeo.uhu.es (R. Pérez-López).

https://doi.org/10.1016/j.marpolbul.2022.114491
Received 7 October 2022; Received in revised form 8 December 2022; Accepted 11 December 2022
Available online 23 December 2022

particulate phases in response to the salinity gradients from fresh- and seawaters (Morris et al., 1986; Bewers and Yeats, 1989; Baeyens et al., 1998; Zhou et al., 2003). In addition to saline mixing, other geochemical processes also occur in estuaries receiving AMD-affected streams, as there is a sharp gradient of pH, from values between 2.5 and 3.5 at the fluvial domain to values close to 8.0 in the marine domain, which occurs in a very short distance. Such a wide variation in pH values can cause elements, which mostly behave conservatively in fluvial courses, to undergo geochemical processes related to acid neutralisation that affect their mobility in marine environments. Although these processes have been simulated using geochemical modelling (Asta et al., 2015), the study of the synergy between hydrochemical and mineralogical information of such reactions in estuarine systems is still in its infancy.

The main objective of this study is to elucidate the main geochemical reactions that occur in estuaries or other coastal sites receiving AMD-affected river waters. These processes significantly control the fluvial flux of elements reaching the oceans. With this objective in mind, classical laboratory mixing experiments were performed to evaluate the conservative or non-conservative behaviour of AMD-related elements during mixing with seawater. Such behaviour was assessed by chemical analysis of the mixing solutions and mineralogical characterisation of the newly-formed phases. As a complementary tool, geochemical modelling was performed with the PHREEQC code to seek understanding between the hydrochemical and mineralogical results (Parkhurst and Appelo, 2013).

2. Materials and methods

2.1. Study site

The Estuary of Huelva is formed by the confluence of the Tinto and Odiel Rivers (SW Spain). Both rivers, strongly affected by AMD, drain a region known geologically as the Iberian Pyrite Belt (IPB), which is one of the most important massive sulfide provinces in the world with original reserves in the order of 1700 Mt. (Sáez et al., 1999). Intense mining activity in the IPB dates back to about 5000 years of history (Davis et al., 2000; Leblanc et al., 2000). The main environmental problem in the IPB is the AMD generation from the surface oxidation of sulfide minerals contained in abandoned mine wastes. These acidic and metal(loid)-rich leachates are drained by the Tinto and Odiel Rivers, causing the total pollution of their waters (e.g., Olías et al., 2006; Nieto et al., 2013). The transfer of acidity and potentially toxic elements to the Estuary of Huelva has been the focus of numerous investigations (e.g., Elbaz-Poulichet et al., 2001; Borrego et al., 2002; Braungardt et al., 2003; Carro et al., 2011; Hierro et al., 2014). Pollution levels are so extreme that both rivers and the estuary can be considered one of the most polluted aquatic systems in the world. The fluvial contribution of contaminants to the Estuary of Huelva for different periods and under different climatic conditions is well known. For example, Olías et al. (2006) calculated the discharge for the period 1995 to 2003 and estimated that both rivers contribute to the estuary >50 % of the total Zn and 10 % of the total Cu transferred globally from the continents to the oceans. The lack of control measures at abandoned IPB mining facilities can also lead to accidental spills of huge volumes of AMD that increase the input of pollutants to the oceans. A clear example is what happened in 2017 in the abandoned La Zarza mining district when the concrete plug of an underground gallery collapsed, suddenly releasing 270,000 m^3 of AMD from an open-pit lake to the Odiel River (Olías et al., 2019). The IPB is hence a local case study but with global environmental implications. At present, the application of some eco-sustainable full-scale passive treatment systems based on alkaline addition has shown to be highly effective in reducing the pollutant load and acidity in abandoned AMD discharges at the IPB (Martínez et al., 2019; Orden et al., 2021). This research focuses on geochemical processes occurring in the Estuary of Huelva; however, it can be extended to other mining districts around the world where AMD streams mix directly with seawater such as King River (Tasmania, Australia; Augustinus et al., 2010), Chonam-ri Creek (Kwangyang, South Korea; Jung et al., 2012), Afon Goch (Anglesey, North Wales; Dean et al., 2013) and Gromolo Torrent (Liguria, North-West Italy; Consani et al., 2017).

2.2. Sampling and estuarine water mixing experiments

Geochemical processes that take place during the progressive interaction of AMD with seawater in the Estuary of Huelva were evaluated in the laboratory to fully control the mass balance and so evaluate reaction-paths responsible for the mobility of contaminants during the mixing. For this purpose, mixing experiments were carried out using different AMD samples from various locations in the IPB. The samples were selected to cover a wide range of geochemical representativeness. Within the Odiel River basin, two samples were taken during the accidental spill from La Zarza pit lake in 2017: in the mine site (La Zarza) and just in the Odiel River before the estuary coinciding with the arrival of the contamination plume (Gibraleón). Within the Tinto River basin, two different samples were collected in 2018: from an underground mine gallery at the Riotinto mining district (Riotinto) and in the Tinto River just before the estuary (Niebla). This also allows making a comparison between the two river basins in terms of the behaviour of pollutants during estuarine mixing and between natural conditions and accidental spills. In the case of the sample from Riotinto, the AMD arises from an underground mine drift with limited oxygen renewal, so high Fe (II) to total Fe ratios are expected, which also allows predicting the redox behaviour of iron in marine environments. Sampling locations can be consulted at KML file of the Supplementary information.

For mixing experiments with AMD from the Odiel River basin, seawater was taken from the ocean coast at a contamination-free underway to study the exclusive effect of the mine spill in the estuary. However, mixing experiments with AMD from the Tinto River basin were carried out using estuarine water within the marine domain. In the field, 5 L of AMD and 25 L of seawater were collected in decontaminated polyethylene containers, previously rinsed with the same sample. Seawater sampling on the ocean coast was carried out using a Niskin bottle from a boat and at a depth of 10 m to avoid possible cross-contamination by the boat. Data on pH, electrical conductivity (EC), oxidation-reduction potential (ORP) and temperature were measured in situ with a Crison MM40+ portable multiparameter instrument. A calibration at three points was performed for both EC and pH (147 μS/cm, 1413 μS/cm, and 12.88 mS/cm and 4.01, 7.00, and 9.21, respectively), while ORP was controlled using two different standard solutions (220 and 470 mV). Samples were immediately transferred to the laboratory where titration experiments were performed by dropwise addition of seawater over an initial volume of unfiltered AMD using a graduated burette under continuous stirring with a magnetic bar. The initial volume of AMD for all experiments depended mainly on the pH of the sample, so the data are expressed as mixing ratios estuarine water to acid mine water. The physicochemical parameters were measured continuously throughout the pH rise to values of 7.0–7.5. Once the titration was finished, the experiments were repeated under the same conditions in order to collect samples of solution at different pH values (from 2.5 to 7.5, in increments of 0.5 pH units). Solid precipitates were collected at pH values of 4.0 and 5.5 in each mixing experiment, and also at pH of 7.5 in the mixing experiment with AMD from Riotinto. These pH values (approx. 4.0, 5.5 and 7.5) coincide with the stability fields for Fe (III), Al and Fe(II) oxyhydroxysulfates, respectively, typical of AMD neutralisation and their precipitation is expected (Nordstrom and Alpers, 1999). In the case of the AMD from Riotinto, the possible precipitation of Fe(II) phases must be considered given the expectedly high Fe (II) concentration in this sample as stated before.

The resulting solutions and precipitates from each mixing experiment were collected for analysis. Two aliquots were subsequently separated in polyethylene vials after filtering through 0.45 μm pore size filters; one for analysis of cation concentrations after being acidified

with 1 % suprapure nitric acid, and another unacidified for anion analysis. The solid precipitate samples for the different pH values were collected on filter paper (0.45 μm of pore size) by filtration of the total amount of the solutions using a vacuum pump. These solid samples were freeze-dried by lyophilization and examined for mineralogical characterisation of newly-formed phases.

2.3. Chemical and mineralogical analyses

Major elements concentrations were determined by Inductively Coupled Plasma-Atomic Emission Spectroscopy (ICP-AES; Jobin Yvon Ultima 2) at the University of Huelva. Trace elements concentrations were determined by Inductively Coupled Plasma-Mass Spectrometry (ICP-MS) with a Thermo Scientific iCAP TQ ICP-MS a the Plateforme AETE-ISO (HydroSciences/OSU OREME, University of Montpellier) without any prior dilution using Kinetic energy Discrimination - Argon Gas Dilution (KED-AGD mode). For trace element determinations, an internal solution containing Be, Sc, Ge, Rh and Ir was added on-line to the samples to correct signal drifts. Estuarine water reference materials for trace metals (SLEW-3 and CASS-6) were also analyzed to check the analytical accuracy. Detection limits were between 0.02 and 0.2 mg/L for major elements and ranged from 0.23 μg/L (Zn) to 3.44 pg/L (La) for trace elements. Detailed information about detection limits and reference material analysis can be found in the Table S1 of the Supplementary information (SI). In addition, anions concentrations were determined using ion chromatography (Dionex DX-120) at the laboratories of the University of Huelva. In mixing experiments with AMD from Tinto River basin, information on Rare Earth Elements and Yttrium (abbreviated as REY) was also obtained and will be discussed in the current study. The Fe(II)/Fe(III) concentrations in mixing experiments with the AMD sample from Riotinto were determined using 1.10 phenanthroline according to standard methods (Tamura et al., 1974) with a Hach DR/890 spectrophotometer.

The solid samples were analyzed by bulk powder X-ray diffraction (XRD) using a Bruker D8 Advance X-ray diffractometer at the University of Huelva. Working conditions were slit fixed at 12 mm, Cu Kα monochromatic radiation, 30 mA and 40 kV, a scan range of 3–65° 2θ, 0.02° 2θ step size and 9.3 s counting time per step. Samples were also examined by FEI QemScan 650F high-resolution Field Emission Environmental Scanning Electron Microscope (SEM) at Center for Scientific Instrumentation at the University of Granada. The samples were mounted on carbon tape, carbon coated, and back-scattered mode was used for high-resolution imaging of the particles and the semi-quantitative chemical composition was examined by energy-dispersive X-ray microanalysis (EDX). The acceleration voltage was set to 20 kV for the data acquisition.

2.4. Geochemical modelling

Speciation-solution and reaction calculations were performed using the geochemical modelling PHREEQC-3.0 code (Parkhurst and Appelo, 2013) and the WATEQ4F thermodynamic database (Ball and Nordstrom, 2001). This database was enlarged with data from Bigham et al. (1996) and Davesne et al. (2010) to account for schwertmannite and green rust solubility, respectively. For geochemical modelling, values of ORP were corrected to obtain Eh values, referenced to the standard hydrogen electrode (Nordstrom and Wilde, 1998). PHREEQC code was used to calculate aqueous speciation of solutions and saturation indices of the solid phases [$SI = \log (IAP / K_S)$, where SI is the saturation index, IAP is the ion activity product and K_S is the solid solubility product]. PHREEQC code was also used to check the quality of the analyses through calculating the charge balance error between cations and anions, which was within 10 % for all the samples.

3. Results and discussion

3.1. Chemical composition of starting solutions

The geochemical characteristics of starting solutions are summarised in Table S2 of the SI. The AMD samples displayed conditions of high acidity and extreme contamination, with pH values of 2.27 (La Zarza), 2.44 (Niebla), 2.49 (Gibraleón) and 2.77 (Riotinto), and electrical conductivities of 8.41, 2.63, 2.90 and 13.5 mS/cm, respectively. As expected from extreme acidity and high electrical conductivity values, AMD solutions contain high concentrations of anions and cations, some of them being potentially toxic pollutants, especially in the samples from the upper part of both river basins; e.g., 31.4 and 13.4 g/L of SO_4, 3908 and 2374 mg/L of Fe and 1865 and 554 mg/L of Al for the AMD from Riotinto and La Zarza, respectively, in addition to other elements such as Zn (841 and 106 mg/L), Cu (286 and 97.6 mg/L), Co (17.0 and 4.80 mg/L), Cd (3.87 and 0.39 mg/L), Ni (1.63 and 3.97 mg/L) and As (763 and 5432 μg/L, respectively). Percentages of Fe(II) relative to total Fe in the AMD from Riotinto are higher than 85 % (Table S2). In addition, the sum of REY concentrations in the latter AMD is 5.77 mg/L. In the other AMD samples, aqueous total Fe is mostly found as Fe(III). On the other hand, seawater showed typical alkaline pH values of 7.64 and 8.22 for estuarine and open seawater, as well as electrical conductivities of 35.6 and 49.1 mS/cm, respectively. In addition, all the contaminants detected in the AMD samples were in negligible abundances in the seawater samples (Table S2), especially in the sample collected in the open sea, and therefore, these samples do not contribute to the resulting concentrations after mixing experiments.

Geochemical modelling results obtained with PHREEQC code are shown in the Table S3 of the SI. According to these simulations, starting AMD solutions were supersaturated with respect to Fe(III) mineral phases such as schwertmannite ($Fe_8O_8(OH)_{4.5}(SO_4)_{1.75}$), ferrihydrite ($Fe(OH)_3$), jarosite ($KFe_3(SO_4)_2(OH)_6$), goethite (FeOOH) and lepidocrocite (FeOOH) (Table S3). Among these minerals, acid drainage precipitates in waters with pH values in the range of 2.8 to 4.5 are predominantly composed of schwertmannite, as suggested by Bigham et al. (1996). As stated before, the spontaneous precipitation of schwertmannite and its high affinity for As could explain the non-conservative character of Fe and As in AMD-affected streams. This is especially significant in the case of the La Zarza spill since the accidental discharge led to a notable increase in flow and element concentrations, also increasing the amount of Fe-rich suspended colloids, likely schwertmannite, within the pollution plume, as observed by Olías et al. (2019). These latter authors found that precipitation and adsorption/coprecipitation processes along the river removed up to 65 % of Fe and 97 % of As in the form of particulate matter before reaching the estuary. In fact, the AMD sample collected for the current study transported suspended colloids within the contamination plume and ochre-coloured precipitates settled to the bottom of the container during the transport of the sample to the laboratory. Given the high amount of suspended particulate matter, titration experiments with this AMD sample also allowed studying the effect of the interaction of particulate matter contaminants with seawater.

3.2. Mixing ratios of estuarine water to acid mine water

The titration curves show the neutralisation of acidity during mixing with seawater (Fig. 1). The respective amounts of seawater and AMD used for each target pH, together with the physicochemical parameters for all samples, are compiled in Table S2. The extreme acidity of the AMD samples implies a slow pH increase even with the addition of large amounts of seawater. Approx. 8.8 mL, 11 mL, 237 mL and 107 mL of seawater were necessary to raise the pH up to 7 for each mL of AMD from Niebla, Gibraleón, Riotinto and La Zarza, in that order. Furthermore, some inflection zones were observed in the titration curves where higher seawater to AMD ratios were required to raise pH values, indicating the occurrence of buffers probably due to changes in aqueous speciation or

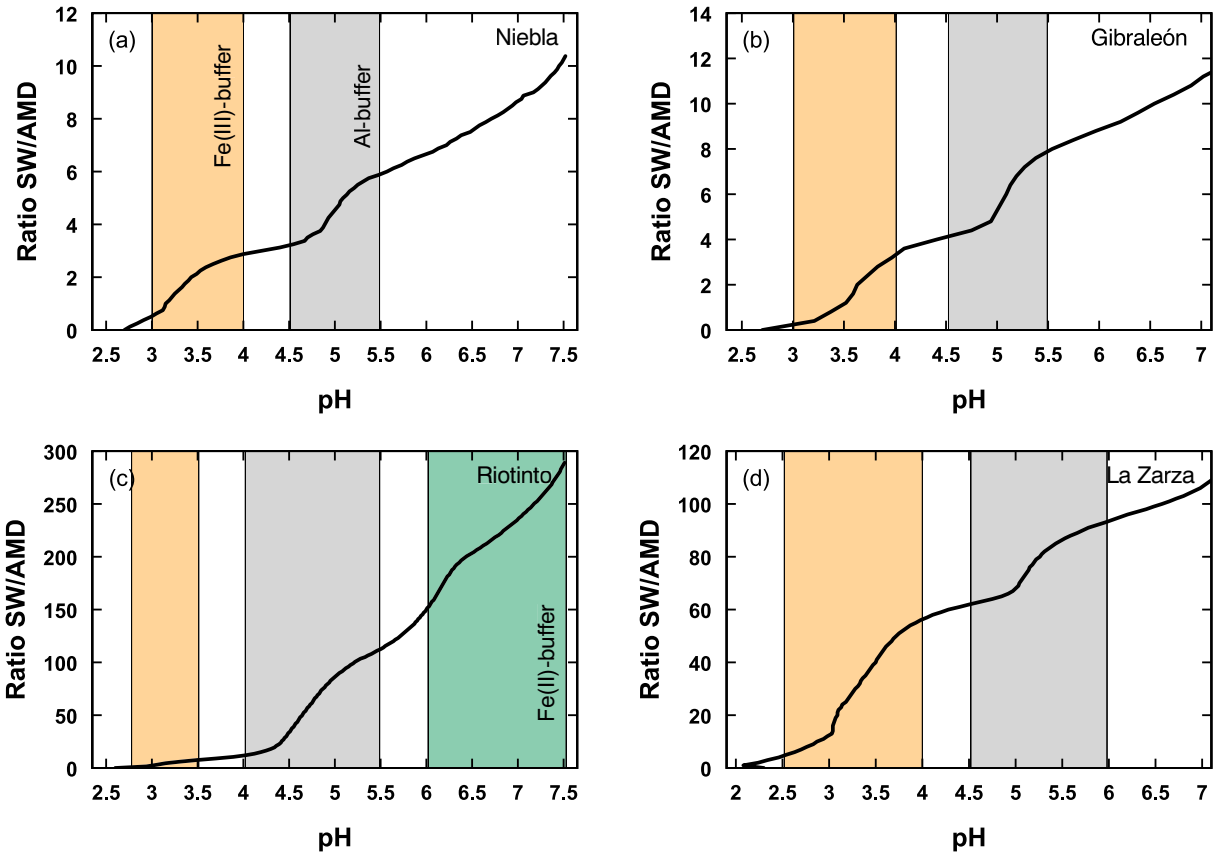

Fig. 1. Evolution of pH during addition of seawater to AMD from (a) Niebla, (b) Gibraleón, (c) Riotinto and (d) La Zarza. Orange, grey and green areas represent different buffers for Fe(III), Al and Fe(II), respectively. (For interpretation of the references to colour in this figure legend, the reader is referred to the web version of this article.)

mineral solubility involving proton release and, thus, hindering pH rise. These buffer zones coincide with solubility changes in Fe(III), Al and Fe (II) due to precipitation of oxyhydroxysulfates as discussed in later sections and, for this reason, they have been named Fe(III)-, Al- and Fe (II)-buffers in Fig. 1. In fact, similar mixing experiments but at extreme net acidity conditions required an order of magnitude more seawater than here to overcome these same buffer barriers and thus reach neutrality due to extremely high Fe and Al concentrations (Lecomte et al., 2017).

3.3. Trends in solution chemistry during mixing experiments

The concentrations observed in the starting AMD decreased significantly from the initial values during the mixing experiments due mainly to dilution by seawater addition. In fact, concentrations observed in the mixing solutions at circumneutral pH are similar to those found in seawater given the high amounts of seawater used in the experiments (Table S2). To evaluate the behaviour of the contaminants during the experimental run subtracting the dilution effect, theoretical concentrations ($[M]_{Theoretical}$) for each target pH value were calculated from the concentrations analyzed in the extreme members, i.e., seawater ($[M]_{SW}$) and AMD ($[M]_{AMD}$), multiplied by the volume fraction of the mixture seawater ($vol.\ fraction_{SW}$) and AMD ($vol.\ fraction_{AMD}$) according to the following equation (Eq. (1)):

$$[M]_{Theoretical} = \left([M]_{SW} \times vol.fraction_{SW}\right) + \left([M]_{AMD} \times vol.fraction_{AMD}\right) \quad (1)$$

Similarity between theoretical and experimental concentrations for a given element during the mixing is indicative that the decrease in concentration is due exclusively to a dilution effect, i.e. such element shows a conservative behaviour. On the contrary, experimental values lower that theoretical concentrations indicate that mineral precipitation also occurs during mixing, i.e. such element shows a non-conservative behaviour.

Evolution with the pH increase of the relationship between the experimental concentrations and those calculated from the theoretical mixing of end-members, in terms of percent similarity, for some major metals such as Fe and Al and trace elements such as As and Cu can be found in the Figs. 2 and 3. The results evidence that these elements exhibited a non-conservative behaviour throughout the seawater mixing experiments, i.e. their concentrations decrease in solution not only by dilution but also by mineral precipitation processes. The first buffer observed in the titration curves (orange bands; Fig. 1) is found at pH values between 2.5 and 4.0 and coincides with the Fe(III) precipitation (Fig. 2), which passes from being 100 % in solution to values below detection limit in the experiments with AMD from Niebla, Gibraleón and La Zarza. Geochemical modelling suggests that solutions in this buffer zone are supersaturated with respect to Fe(III) phases such as schwertmannite, ferrihydrite, jarosite, goethite and lepidocrocite (Table S3). As observed in the reactions showed in Table S3, Fe(III) precipitation releases protons that would counteract the pH increase by seawater addition and buffer the pH until all of the Fe(III) in solution is depleted, completing the process of Fe removal that naturally begins with the spontaneous precipitation in the starting AMD. The second buffer observed in the titration curves (grey bands; Fig. 1) is recorded at pH values between 4.5 and 6.0 and corresponds to the total Al precipitation in all mixing experiments (Fig. 3). According to geochemical calculations, these observations were consistent with Al hydrolysis and subsequent precipitation, buffering the pH. In fact, solutions at this pH range were supersaturated with respect to Al phases such as basaluminite ($Al_4(OH)_{10}SO_4$), gibbsite ($Al(OH)_3$), alunite ($KAl_3(SO_4)_2(OH)_6$),

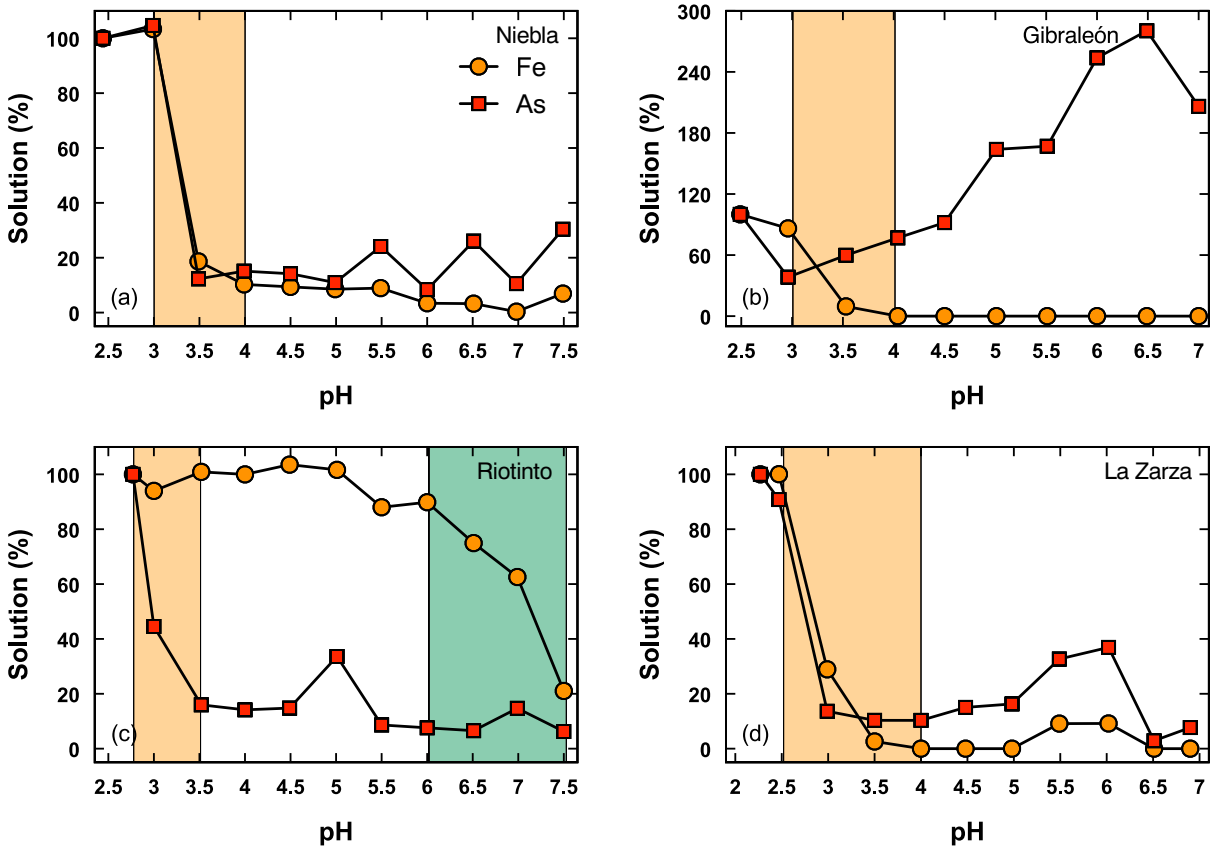

Fig. 2. Evolution of Fe and As percentages during addition of seawater to AMD from (a) Niebla, (b) Gibraleón, (c) Riotinto and (d) La Zarza. Percentages refer to the ratio between the experimental concentrations and the concentrations calculated from theoretical mixing of end-members (see Eq. (1)).

boehmite (AlOOH) and diaspore (AlOOH) (Table S3). These observations are consistent with the different first hydrolysis constants of Fe(III) and Al, with pK values of 2.2 and 5.0, respectively, as discussed in Nordstrom and Ball (1986) and Bigham and Nordstrom (2000).

In the starting AMD sample from Riotinto, around 85 % of total Fe is as Fe(II) as stated before (Table S2), which explains why the buffer corresponding to Fe(III) precipitation is negligible (orange band) compared to the buffer corresponding to Fe(II) precipitation at higher pH values of 6.0–7.5 (green band; Figs. 1c and 2c). In fact, according to the evolution of Fe(II)/Fe(III) in this experiment (Table S2), Fe(III) concentrations drastically decrease at pH around 3.5, whereas percentages of Fe(II) in solution at that time reach values above 95 % which are maintained until all aqueous Fe(II) is removed from solution at pH higher than 6.5. In this case, geochemical modelling showed that the solutions are supersaturated with respect to green rust phases ($Fe_6(OH)_{12}(SO_4)$) (Table S3). The minimum solubility of divalent metals requires higher pH values than for trivalent metals (Cortina et al., 2003) and this Fe(III)/Fe(II) partitioning has been previously described in other AMD titration experiments with alkaline reagents (Carrero et al., 2015).

Ferric iron removal is concomitant with the depletion of most of the As from solutions in the first buffer at pH between 2.5 and 4.0, even also in the case of the AMD sample from Riotinto where Fe precipitation occurs mainly at higher pH values associated with the Fe(II) buffer (Fig. 2). However, there seems to be an increase in the As concentration in solution at higher pH values. This increase is not so clear in the mixing experiments with AMD from Niebla or La Zarza where concentrations are very close to detection limit of ICP-MS due to a huge dilution; however, experimental As concentrations progressively increase with pH in the experiment with AMD from Gibraleón, reaching values even higher than those deduced from the theoretical mixing (Fig. 2). This increase in As concentration could be associated with a possible instability of Fe(III) precipitates in the marine environment. On the other hand, Al precipitation from solution at pH between 4.5 and 6.0 could also remove other metals such as Cu in the experiments with AMD from Niebla, Gibraleón and La Zarza (Fig. 3). Surprisingly, Cu removal by Al precipitation does not occur in the experiment with AMD from Riotinto, which shows a conservative behaviour over the entire pH range. It seems that the oxidation state of the AMD from Riotinto with high Fe(II) ratios could also play a role on the mobility of Cu during estuarine mixing. The behaviour of As and Cu in relation to Fe(III) and Al precipitates, respectively, will be discussed in detail later once mineralogical characterisation of the buffer zones has been described. Along with Cu, removal of REY during the mixing also occurs almost concomitantly with the removal of Al (Fig. 3).

Other contaminants such as S, Zn, Cd, Ni and Co show a conservative behaviour throughout the whole mixing experiments, i.e., their experimental concentrations can be deduced from the theoretical mixing of end-members since these elements does not participate in mineral precipitation processes or their participation is negligible (Fig. 4).

3.4. Newly-formed solid-phase characterisation

The chemical analyses of the mixing solutions showed that major elements such as Fe and Al were largely removed from the solutions with increasing pH, implying that their concentrations decreased by precipitation processes, buffering the pH. Thus, the characterisation of the newly-formed solids was required to provide a complete picture of the geochemical processes controlling contaminant mobility during mixing of AMD solutions with seawater. The XRD spectra revealed that newly-formed precipitates during the Fe(III) buffer correspond to schwertmannite; whereas Al precipitates as basaluminite during the Al buffer.

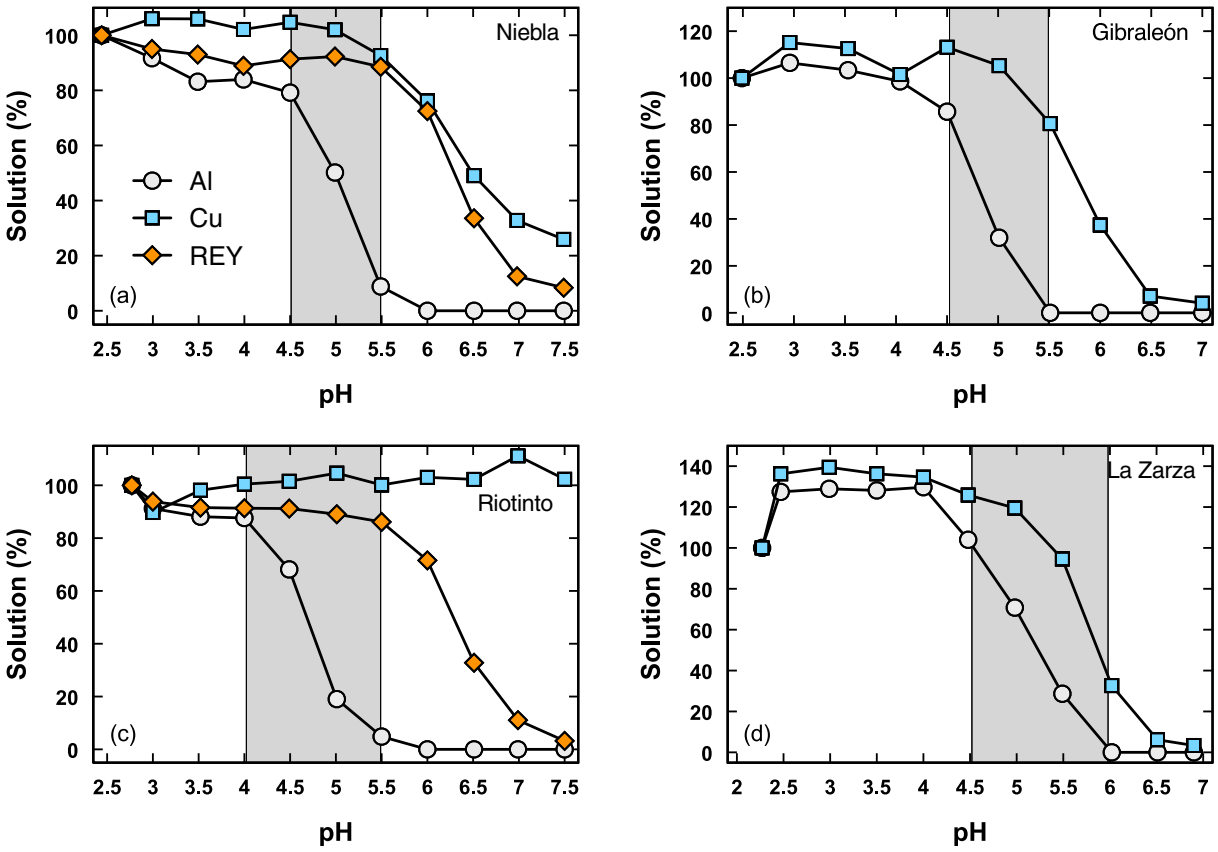

Fig. 3. Evolution of Al and Cu percentages during addition of seawater to AMD from (a) Niebla, (b) Gibraleón, (c) Riotinto and (d) La Zarza. REY percentages were also shown in the experiments with AMD from (a) Niebla and (c) Riotinto. Percentages refer to the ratio between the experimental concentrations and the concentrations calculated from theoretical mixing of end-members (see Eq. (1)).

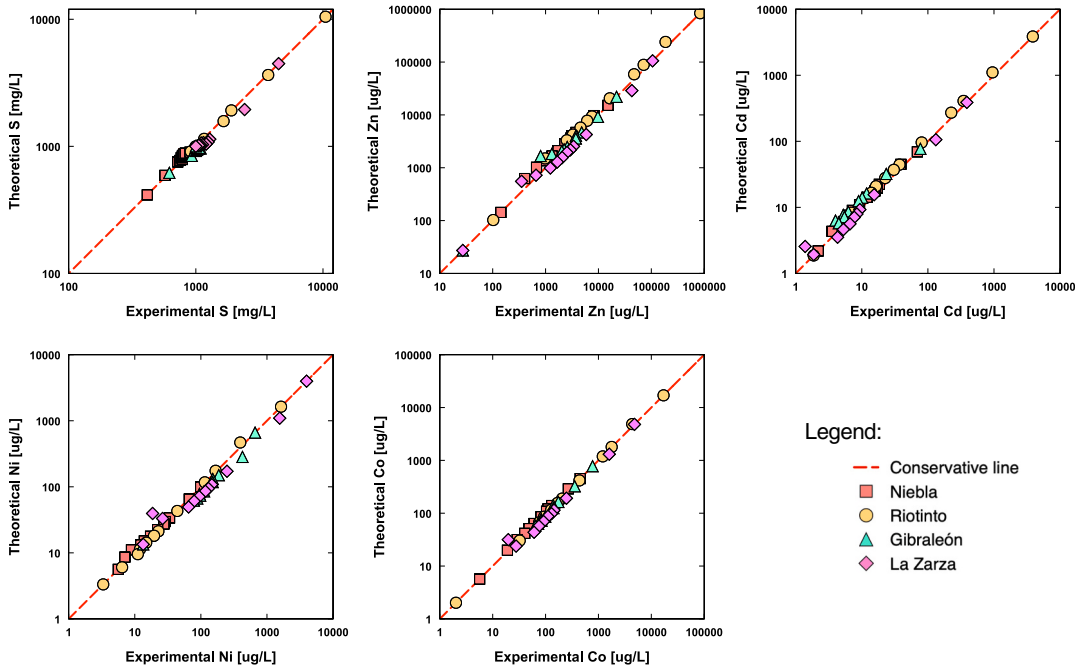

Fig. 4. Correlation between the experimental concentrations and the concentrations calculated from theoretical mixing of end-members for all AMD samples. Red line represents the conservative behaviour, i.e., those elements plotting on the conservative line do not precipitate during acid neutralisation. (For interpretation of the references to colour in this figure legend, the reader is referred to the web version of this article.)

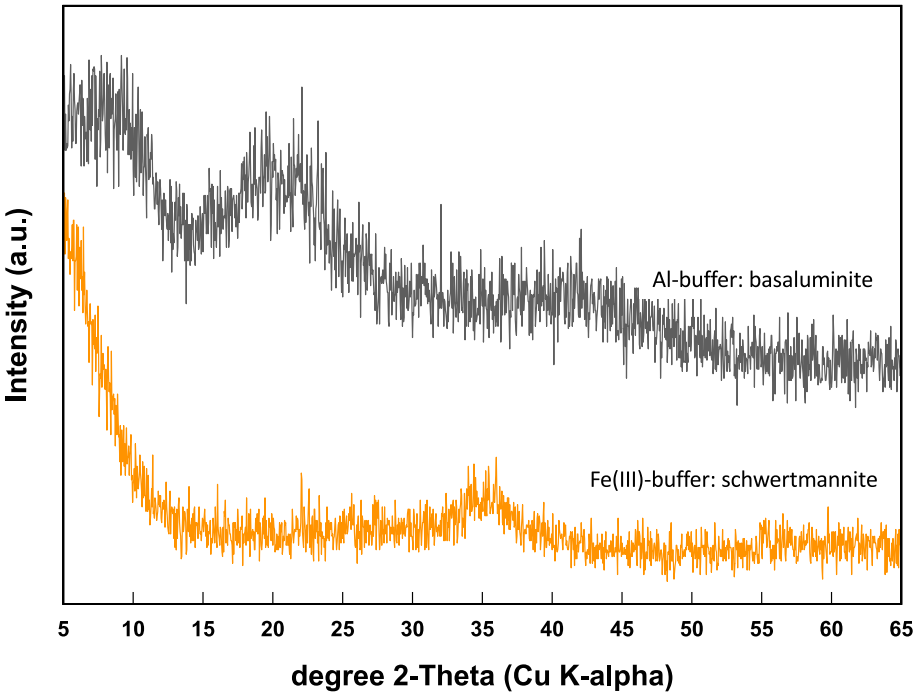

Fig. 5. Representative XRD spectra revealing precipitation of schwertmannite in the Fe(III) buffer and basaluminite in the Al buffer.

Both minerals are poorly crystalline as suggested by their typical XRD spectra shown in Fig. 5. Moreover, precipitation of these minerals is consistent with the nature of the phases suggested by the geochemical modelling with PHREEQC, being also the most stable phases governing hydrochemistry and mineralogy in AMD-affected river systems (Bigham et al., 1996; Nordstrom and Alpers, 1999). Accordingly, schwertmannite may control As mobility in solution, while basaluminite may control Cu and REY mobility. Precipitation of Fe(II) at pH higher than 6.0–7.5 in the mixing experiment with AMD from Riotinto may occur in the form of green rust as suggested by the modelling (Table S3). However, these precipitates are highly unstable and may transform to ferric oxyhydroxide even during XRD analysis (Carrero et al., 2015).

SEM-EDX images revealed that the newly-formed schwertmannite precipitates are submicrometric agglomerates of globular phases chemically composed of S and Fe (Fig. 6a). Some images reveal the typical hedgehog morphology of schwertmannite (Fig. 6b). Identification of other elements such as As in schwertmannite was not possible due likely to difficulties measuring concentrations close to the detection limit. On the other hand, SEM-EDX confirmed that basaluminite was present as micrometric particles composed of S and Al (Fig. 6c). Other metals such as Cu were detected together with Al in the basaluminite aggregates (Fig. 6d), supporting the similar chemical evolution during the mixing experiments, with removal of both elements within the same pH range (Fig. 4). The EDX spectra revealed lower concentration of S in relation to Fe and Al in schwertmannite and basaluminite (Fig. 6d), respectively, which is consistent with the chemical composition of both phases. This noticeably low amount of sulfate incorporated into the oxyhydroxysulfates, together with the high sulfate concentrations in the starting AMD solutions, would explain that sulfate behaves conservatively in solution despite the precipitation of these newly-formed phases during mixing.

4. Environmental implications

The precipitation sequence of schwertmannite (and its affinity for As at low pH values) followed by basaluminite (and its affinity for Cu and REY) as the pH increases by alkaline addition has been previously described both in mixing between acidic river and pristine waters (Lozano et al., 2020) and in treatment systems of acidic drainages (Macías et al., 2012; Orden et al., 2021). In this sequence, basaluminite precipitates at pH 4.5–6.0 when iron is totally removed from the solution by previous schwertmannite precipitation at pH 2.5–4.0. Nevertheless, iron concentrations in the AMD-affected fluvial courses from the IPB are so high that schwertmannite precipitation buffers the pH to low values and basaluminite precipitation in natural systems is consequently anecdotal. In fact, Al precipitation is only limited to punctual secondary courses where the pK of Al hydrolysis is triggered. On the contrary, a wide pH range is observed in the Estuary of Huelva and Al precipitation as basaluminite must be of greater importance than in fluvial systems. Although other phases of Al had been suggested in previous studies based exclusively on geochemical modelling of estuarine mixing (Asta et al., 2015), the results obtained in this study denote, for the first time, the importance of basaluminite precipitation in Al fluxes to oceans. On the other hand, other pollutants such as Zn, Cd, Co and Ni have a clearly conservative behaviour reaching open sea conditions dissolved in the water, being their concentration only affected by dilution.

Arsenic adsorption capacity of schwertmannite depends mainly on the surface charge of the mineral, as discussed above. In acidic conditions schwertmannite surfaces are protonated and hence positively charged, whereas the main aqueous As species for the whole pH range is in the form of oxyanion ($H_2AsO_4^-$) according to geochemical modelling with PHREEQC. Both aspects explain the high affinity of As for schwertmannite by adsorption. However, the schwertmannite surface is dehydroxylated and negatively charged in alkaline conditions. The pH at which the surface has an equal amount of positive and negative adsorption sites is called the point of zero charge. At pH values above the point of zero charge, schwertmannite surface becomes negatively charged and As desorption is expected. The change in the surface properties of schwertmannite precipitates with increasing pH may explain the increase in dissolved As concentrations during seawater addition, especially in the AMD sample from Gibraleón which contains high concentrations of suspended schwertmannite-rich material in the starting sample. Therefore, a part of the As that reaches the estuary is added to the conservative pollutants, i.e. S, Zn, Cd, Ni and Co, ending up in the Atlantic Ocean.

Concerning basaluminite, its precipitation seems to play a

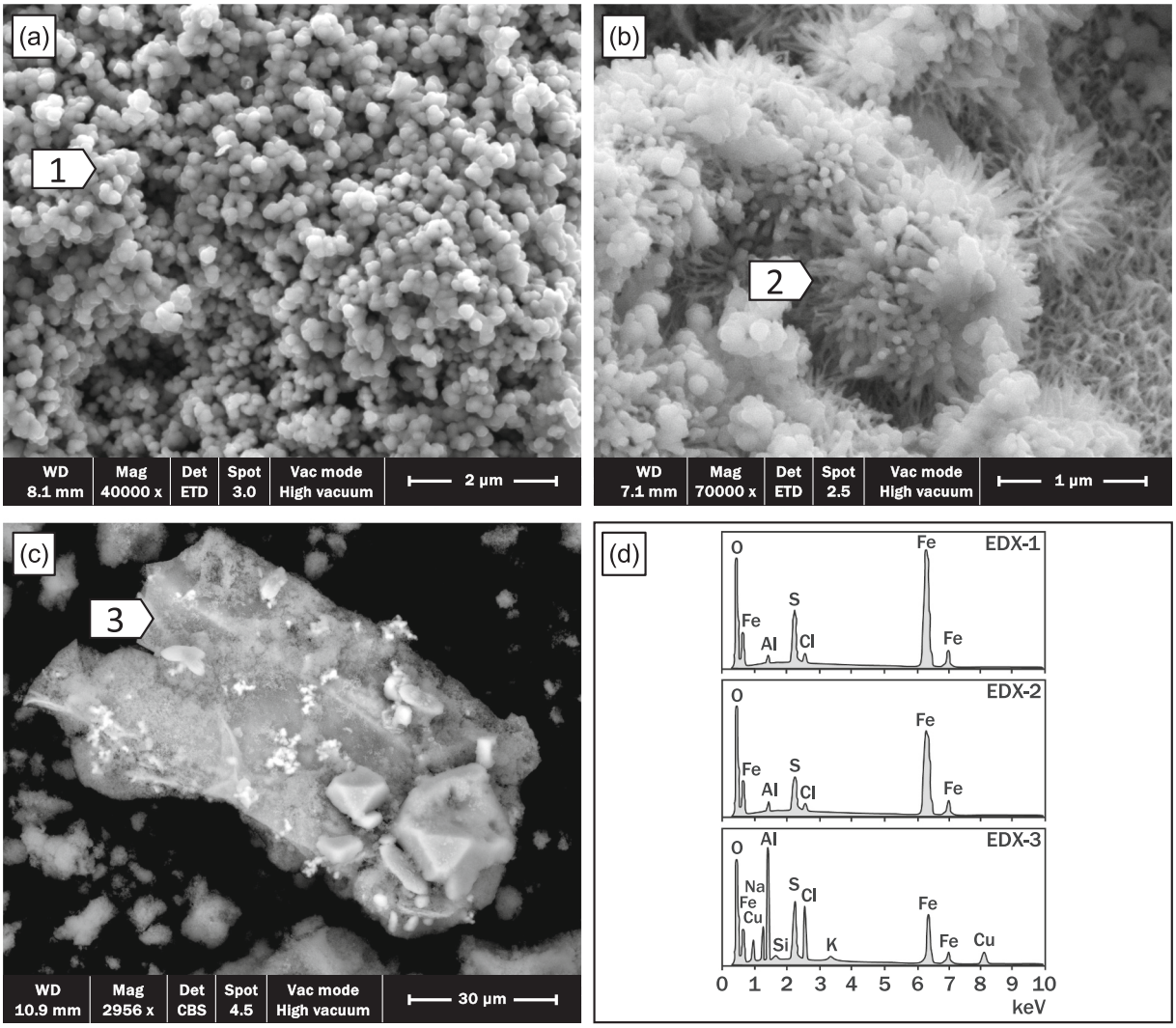

Fig. 6. Representative SEM images of newly-formed precipitates collected during all mixing experiments: (a, b) schwertmannite in Fe(III) buffer, (c) basaluminite in Al buffer and (d) some EDX spectra of points of interest.

fundamental role on the removal of Cu and REY. Nevertheless, the Cu and REY concentrations in the mixing experiments continue to decrease after Al is practically absent in solution (Fig. 3), suggesting that another retention mechanism such as minor precipitation of oxyhydroxides or fluorides cannot be ruled out (Ayora et al., 2016). It is remarkable that basaluminite seems to control the mobility of Cu only in Fe(III)-rich AMD solutions since Cu behaves conservatively despite aluminum precipitation in Fe(II)-rich AMD solutions emerging under oxygen-limited conditions, as is the case of the AMD sample from Riotinto. This conservative behaviour for Cu under oxygen-limited conditions could be related to its aqueous speciation. According to geochemical modelling, much of the Cu in solution during the mixing experiment with AMD of Riotinto over the whole pH range is found as Cu(I), mainly as $CuCl_3^{-2}$. In this sense, Matocha et al. (2005) demonstrated that Cu(II) is rapidly reduced to Cu(I) in presence of Fe(II) under anoxic conditions in solutions with high Cl concentrations, which stabilizes Cu(I) in solution against mineral precipitation. The important role of reduced iron (Fe(II)) on reductive transformation and stabilization in solution of Cu would confirm the findings observed in the current study. This process may be important in estuarine marsh environments with high organic matter decomposition where high dissolved Fe(II) concentrations can accumulate (Pérez-López et al., 2018). Instead, Cu(II) is the majority species in the rest of experiments with Fe(III)-rich AMD solutions, which would explain its removal during basaluminite precipitation.

This analysis of the behaviour of contaminants with increasing pH, simulating seawater mixing in the estuary, can be contrasted with earlier studies carried out in the coastal zone. For example, Spivack et al. (1983), Boyle et al. (1985) and Sherrell and Boyle (1988) reported the first observations on pollutant enrichment in the Gulf of Cadiz in the 1980s during an oceanographic expedition organised by the Woods Hole Oceanographic Institution in Massachusetts. These authors concluded that the seawater of the Gulf of Cadiz shelf is particularly enriched in dissolved metal(loid)s, mainly Zn, Cd and As, compared to other coastal waters. It was originally thought that this enrichment was due to a process of upwelling from deep ocean areas as well as metal sequestration in the Gulf of Cadiz (Van Geen et al., 1991). However, Elbaz-Poulichet and Leblanc (1996) were the first authors who, years later, established that the true source of the contaminants came from two secondary fluvial watercourses, Tinto and Odiel Rivers, and later confirmed this theory by detecting the anomaly in the ocean (Van Geen et al., 1997). These observations coincide with the results of the present investigation, which establishes a conservative behaviour for most of the contaminants from the AMD during estuarine mixing. This conservative behaviour would explain that these elements freely reach the Atlantic Ocean and are distributed throughout the Gulf of Cadiz due to ocean currents.

5. Conclusions

Acid mine drainage (AMD) leachates from abandoned mining districts at the Iberian Pyrite Belt (IPB) discharges, up to day, directly into the Estuary of Huelva (SW Spain) via the Tinto and Odiel Rivers. Different geochemical processes alter the concentrations and influence the mobility of the contaminants contained in the AMD during mixing with alkaline seawater. The current research reports two main conclusions through experimental and theoretical simulations of mixing of AMD with seawater: a) the high acidity of the AMD hinders the rise of the pH requiring enormous amounts of seawater to achieve circumneutral pH values, and b) most of the potentially toxic contaminants including Zn, Cd, Ni, Co and S behave conservatively, whereas Fe and Al decrease significantly with increasing pH by sequential precipitation of first schwertmannite followed by basaluminite. Arsenic participates in sorption processes in schwertmannite, whereas Cu and REY are removed by basaluminite. However, the change in the surface properties of schwertmannite at higher pH values could lead to the instability and release of As, being a sink in acidic conditions but a source of contamination when the newly-formed precipitates reach the marine conditions. Our findings have provided important insight into the problematic of the AMD worldwide and, more importantly, into the pollution of the Estuary of Huelva by mining contaminants. The potentially toxic elements that remain mobile after reaching the estuary, finally end up to the Atlantic Ocean contributing significantly to the total pollutant loads and threatening the environmental conditions of coastal areas. It is, therefore, urgent to adopt effective restoration measures to minimize the impact of the AMD discharges on the estuarine environment and subsequently on the Atlantic Ocean, as well as of other mining districts worldwide where AMD streams reach coastal regions.

CRediT authorship contribution statement

Rafael Pérez-López: Conceptualization, Writing – original draft, Writing – review & editing, Visualization, Supervision, Funding acquisition. **Ricardo Millán-Becerro:** Methodology, Software, Writing – review & editing. **María Dolores Basallote:** Conceptualization, Investigation, Writing – review & editing. **Sergio Carrero:** Writing – review & editing. **Annika Parviainen:** Methodology, Resources, Writing – review & editing. **Rémi Freydier:** Methodology, Resources, Writing – review & editing. **Francisco Macías:** Investigation, Writing – review & editing. **Carlos R. Cánovas:** Investigation, Writing – review & editing.

Declaration of competing interest

The authors declare that they have no known competing financial interests or personal relationships that could have appeared to influence the work reported in this paper.

Data availability

Data will be made available on request.

Acknowledgements

This work was supported by the Spanish Ministry of Science and Innovation under the research project TRAMPA (PID2020-119196RB-C21). C.R. Cánovas, A. Parviainen and M.D. Basallote also acknowledge the Spanish Ministry of Science and Innovation for the Postdoctoral Fellowships granted under application references RYC2019-027949-I, IJCI-2016-27412 and IJC2018-035056-I, respectively. We would also like to thank Dr. Geoff MacFarlane for the editorial handling and two anonymous reviewers for the support and comments that significantly improved the quality of the original paper. Funding for open access charge: Universidad de Huelva/CBUA.

Appendix A. Supplementary data

Supplementary data associated with this article can be found in the online version at https://doi.org/10.1016/j.marpolbul.2022.114491. These data include the Google map of the most important areas described in this article.

References

Ayora, C., Macías, F., Torres, E., Lozano, A., Carrero, S., Nieto, J.M., Pérez-López, R., Fernández-Martínez, A., Castillo-Michel, H., 2016. Recovery of rare earth elements and yttrium from passive-remediation systems of acid mine drainage. Environ. Sci. Technol. 2016 (50), 8255–8262. https://pubs.acs.org/doi/10.1021/acs.est.6b02084.

Acero, P., Ayora, C., Torrentó, C., Nieto, J.M., 2006. The behavior of trace elements during schwertmannite precipitation and subsequent transformation into goethite and jarosite. Geochim. Cosmochim. Acta 70, 4130–4139. https://doi.org/10.1016/j.gca.2006.06.1367.

Asta, M.P., Calleja, M.Ll., Pérez-López, R., Auqué, L.F., 2015. Major hydrogeochemical processes in an acid mine drainage affected estuary. Mar. Pollut. Bull. 91, 295–305. https://doi.org/10.1016/j.marpolbul.2014.11.023.

Augustinus, P., Barton, C.E., Zawadzki, A., Harle, K., 2010. Lithological and geochemical record of mining-induced changes in sediments from Macquarie Harbour, southwest Tasmania, Australia. Environ. Earth Sci. 61, 625–639. https://doi.org/10.1007/s12665-009-0377-x.

Baeyens, W., Elskens, M., Gillain, G., Goeyens, L., 1998. Biogeochemical behaviour of Cd, Cu, Pb and Zn in the Scheldt estuary during the period 1981–1983. Hydrobiologia 366, 15–44. https://doi.org/10.1007/978-94-017-3573-5_2.

Ball, J.W., Nordstrom, D.K., 2001. User's manual for WATEQ4F with revised thermodynamic database and test cases for calculating speciation of major, trace and redox elements in natural waters. U.S. Geol. Surv. Water-Resour. Invest. Rep. 91–183.

Bewers, J., Yeats, P.A., 1989. Transport of river-derived trace metals through the coastal zone. Neth. J. Sea Res. 23 (4), 359–368. https://doi.org/10.1016/0077-7579(89)90020-3.

Bigham, J.M., Schwertmann, U., Carlson, L., Murad, E., 1990. A poorly crystallized oxyhydroxysulfate of iron formed by bacterial oxidation of Fe(II) in acid mine waters. Geochim. Cosmochim. Acta 54 (10), 2743–2758. https://doi.org/10.1016/0016-7037(90)90009-A.

Bigham, J.M., Carlson, L., Murad, E., 1994. Schwertmannite, a new iron oxyhydroxysulphate from Pyhasalmi, Finland, and other localities. Miner. Mag. 58 (4), 641–648. https://doi.org/10.1180/minmag.1994.058.393.14.

Bigham, J.M., Schwertmann, U., Traina, S.J., Winland, R.L., Wolf, M., 1996. Schwertmannite and the chemical modeling of iron in acid sulfate waters. Geochim. Cosmochim. Acta 60, 2111–2121. https://doi.org/10.1016/0016-7037(96)00091-9.

Bigham, J.M., Nordstrom, D.K., 2000. Iron and aluminum hydroxysulfates from acid sulfate waters. Rev. Mineral. Geochem. 40, 351–403. https://doi.org/10.2138/rmg.2000.40.7.

Borrego, J., Morales, J.A., de la Torre, M.L., Grande, J.A., 2002. Geochemical characteristics of heavy metal pollution in surface sediments of the Tinto and Odiel river estuary (southwestern Spain). Environ. Geol. 41, 785–796. https://doi.org/10.1007/s00254-001-0445-3.

Boyle, E.A., Chapnick, S.D., Bai, X.X., Spivack, A.J., 1985. Trace metal enrichments in the Mediterranean Sea. Earth Planet. Sci. Lett. 74, 405–419. https://doi.org/10.1016/S0012-821X(85)80011-X.

Braungardt, C.B., Achterberg, E.P., Elbaz-Poulichet, F., Morley, N.H., 2003. Metal geochemistry in a mine-polluted estuarine system in Spain. Appl. Geochem. 18, 1757–1771. https://doi.org/10.1016/S0883-2927(03)00079-9.

Caraballo, M.A., Rimstidt, J.D., Macías, F., Nieto, J.M., Hochella Jr., M.F., 2013. Metastability, nanocrystallinity and pseudo-solid solution effects on the understanding of schwertmannite solubility. Chem. Geol. 360–361, 22–31. https://doi.org/10.1016/j.chemgeo.2013.09.023.

Carrero, S., Pérez-López, R., Fernandez-Martinez, A., Cruz-Hernández, P., Ayora, C., Poulain, A., 2015. The potential role of aluminium hydroxysulphates in the removal of contaminants in acid mine drainage. Chem. Geol. 417, 414–423. https://doi.org/10.1016/j.chemgeo.2015.10.020.

Carro, B., Borrego, J., López-González, N., Grande, J.A., Gómez, T., de la Torre, M.L., Valente, T., 2011. Impact of acid mine drainage on the hydrogeochemical characteristics of the Tinto-Odiel estuary (SW Spain). J. Iberian Geol. 37, 87–96. https://doi.org/10.5209/rev_JIGE.2011.v37.n1.6.

Consani, S., Carbone, C., Dinelli, E., Balić-Žunić, T., Cutroneo, L., Capello, M., Salviulo, G., Lucchetti, G., 2017. Metal transport and remobilisation in a basin affected by acid mine drainage: the role of ochreous amorphous precipitates. Environ. Sci. Pollut. Res. 24, 15735–15747. https://doi.org/10.1007/s11356-017-9209-9.

Cortina, J.L., Lagreca, I., De Pablo, J., Cama, J., Ayora, C., 2003. Passive in situ remediation of metal-polluted water with caustic magnesia: evidence from column experiments. Environ. Sci. Technol. 37, 1971–1977. https://doi.org/10.1021/es026018m.

Courtin-Nomade, A., Bril, H., Neel, C., Lenain, J.F., 2003. Arsenic in iron cements developed within tailings of a former metalliferous mine - Enguialès, Aveyron, France. Appl. Geochem. 18, 395–408. https://doi.org/10.1016/S0883-2927(02)00098-7.

Davesne, E., Dideriksen, K., Christiansen, B.C., Sonne, M., Ayala-Luis, K.B., Koch, C.B., Hansen, H.C.B., Stipp, S.L.S., 2010. Free energy of formation for green rust sodium sulphate (NaFeII6FeIII3(OH)18(SO4)2(s)). Geochim. Cosmochim. Acta 74, 6451–6467. https://doi.org/10.1016/j.gca.2010.08.015.

Davis Jr., R.A., Welty, A.T., Borrego, J., Morales, J.A., Pendón, J.G., Ryan, J.G., 2000. Rio Tinto estuary (Spain): 5000 years of pollution. Environ. Geol. 39, 1107–1116. https://doi.org/10.1007/s002549900096.

Dean, A.P., Lynch, S., Rowland, P., Toft, B.D., Pittman, J.K., White, K.N., 2013. Natural wetlands are efficient at providing long-term metal remediation of freshwater systems polluted by acid mine drainage. Environ. Sci. Technol. 2013 (47), 12029–12036. https://doi.org/10.1021/es4025904.

Elbaz-Poulichet, F., Leblanc, M., 1996. Transfert de métaux d'une province minière à l'océan par des fleuves acides (Rio Tinto, Espagne). C.RAcad. Sci. Paris 322, 1047–1052. http://pascal-francis.inist.fr/vibad/index.php?action=getRecordDetail&idt=3099594.

Elbaz-Poulichet, F., Braungardt, C., Achterberg, E., Morley, N., Cossa, D., Beckers, J.M., Nomérange, P., Cruzado, A., Leblanc, M., 2001. Metal biogeochemistry in the Tinto-Odiel rivers (Southern Spain) and in the Gulf of Cadiz: a synthesis of the results of TOROS project. Cont. Shelf Res. 21, 1961–1973. https://doi.org/10.1016/S0278-4343(01)00037-1.

Fernandez-Martinez, A., Timon, V., Román-Ross, G., Cuello, G.J., Daniels, J.E., Ayora, C., 2010. The structure of schwertmannite, a nanocrystalline iron oxyhydroxysulfate. Am. Mineral. 95, 1312–1322. https://doi.org/10.2138/am.2010.3446.

Fukushi, K., Sasaki, M., Sato, T., Yanase, N., Amano, H., Ikeda, H., 2003. A natural attenuation of arsenic in drainage from an abandoned arsenic mine dump. Appl. Geochem. 18, 1267–1278. https://doi.org/10.1016/S0883-2927(03)00011-8.

Hierro, A., Olías, M., Ketterer, M.E., Vaca, F., Borrego, J., Cánovas, C.R., Bolívar, J.P., 2014. Geochemical behavior of metals and metalloids in an estuary affected by acid mine drainage (AMD). Environ. Sci. Pollut. Res. 21, 2611–2627. https://doi.org/10.1007/s11356-013-2189-5.

Jung, H.B., Yun, S.T., Kwon, J.S., Zheng, Y., 2012. Role of iron colloids in copper speciation during neutralization in a coastal acid mine drainage, South Korea: insight from voltammetric analyses and surface complexation modeling. J. Geochem. Explor. 112, 244–251. https://doi.org/10.1016/j.gexplo.2011.09.002.

Lambeth, R.H., 1999. Natural attenuation of acidic drainage from sulfidic tailings at a site in Washington State. In: Filipek, L.H., Plumlee, G.S. (Eds.), Soc. Econ. Geol, 6B, pp. 479–491. https://doi.org/10.5382/Rev.06.23.

Leblanc, M., Morales, J.A., Borrego, J., Elbaz-Poulichet, F., 2000. A 4500 years old mining pollution in Spain. Econ. Geol. 95, 655–662. https://doi.org/10.2113/gsecongeo.95.3.655.

Lecomte, K.L., Sarmiento, A.M., Borrego, J., Nieto, J.M., 2017. Rare earth elements mobility processes in an AMD-affected estuary: Huelva Estuary (SW Spain). Mar. Pollut. Bull. 121, 282–291. https://doi.org/10.1016/j.marpolbul.2017.06.030.

Lozano, A., Ayora, C., Macías, F., León, R., Gimeno, M.J., Auqué, L., 2020. Geochemical behavior of rare earth elements in acid drainages: modeling achievements and limitations. J. Geochem. Explor. 216, 106577 https://doi.org/10.1016/j.gexplo.2020.106577.

Macías, F., Caraballo, M.A., Nieto, J.M., Rötting, T.S., Ayora, C., 2012. Natural pretreatment and passive remediation of highly polluted acid mine drainage. J. Environ. Manag. 104, 93–100. https://doi.org/10.1016/j.jenvman.2012.03.027.

Martínez, N.M., Basallote, M.D., Meyer, A., Cánovas, C.R., Macías, F., Schneider, P., 2019. Life cycle assessment of a passive remediation system for acid mine drainage: towards more sustainable mining activity. J. Clean. Prod. 211, 1100–1111. https://doi.org/10.1016/j.jclepro.2018.11.224.

Matocha, C.J., Karathanasis, A.D., Rakshit, S., Wagner, K.M., 2005. Reduction of copper (II) by iron(II). J. Environ. Qual. 34, 1539–1546. https://doi.org/10.2134/jeq2005.0002.

Morris, A.W., Bale, A.J., Howland, R.J., Millward, G.E., Ackroyd, D.R., Loring, D.H., Rantala, R.T.T., 1986. Sediment mobility and its contribution to trace metal cycling and retention in a macrotidal estuary. Water Sci. Technol. 18, 111–119. https://doi.org/10.2166/wst.1986.0186.

Nieto, J.M., Sarmiento, A.M., Cánovas, C.R., Olías, M., Ayora, C., 2013. Acid mine drainage in the Iberian Pyrite Belt: 1. Hydrochemical characteristics and pollutant load of the Tinto and Odiel Rivers. Environ. Sci. Pollut. Res. Int. 20, 7509–7519. https://doi.org/10.1007/s11356-013-1634-9.

Nordstrom, D.K., Ball, J.W., 1986. The geochemical behavior of aluminum in acidified surface waters. Science 232, 54–56. https://doi.org/10.1126/science.232.4746.54.

Nordstrom, D.K., Wilde, F.D., 1998. Reduction-oxidation potential (electrode method), section 6.5, chapter A6. In: National Field Manual for the Collection of Water-Quality Data, p. 20. https://doi.org/10.3133/twri09A6.5.

Nordstrom, D.K., Alpers, C.N., 1999. Geochemistry of acid mine waters. In: Plumlee, G. S., Logsdon, M. (Eds.), Soc. Econ. Geol, 6A, pp. 133–160.

Nordstrom, D.K., 2011. Hydrogeochemical process governing the origin, transport and fate of major and trace elements from mine wastes and mineralized rock to surface waters. Appl. Geochem. 26, 1777–1791. https://doi.org/10.1016/j.apgeochem.2011.06.002.

Olías, M., Cánovas, C.R., Nieto, J.M., Sarmiento, A.M., 2006. Evaluation of the dissolved contaminant load transported by the Tinto and Odiel rivers (South West Spain). Appl. Geochem. 21, 1733–1749. https://doi.org/10.1016/j.apgeochem.2006.05.009.

Olías, M., Cánovas, C.R., Basallote, M.D., Macías, F., Pérez-López, R., Moreno, González R., Millán-Becerro, R., Nieto, J.M., 2019. Causes and impacts of a mine water spill from an acidic pit lake (Iberian Pyrite Belt). Environ. Pollut. 250, 127–136. https://doi.org/10.1016/j.envpol.2019.04.011.

Orden, S., Macías, F., Cánovas, C.R., Nieto, J.M., Pérez-López, R., Ayora, C., 2021. Eco-sustainable passive treatment for mine waters: full-scale and long-term demonstration. J. Environ. Manag. 280, 111699 https://doi.org/10.1016/j.jenvman.2020.111699.

Parkhurst, D.L., Appelo, C.A.J., 2013. Description of input and examples for PHREEQC version 3—a computer program for speciation, batch-reaction, one-dimensional transport, and inverse geochemical calculations. In: US Geological Survey Techniques and Methods, Book 6, chap A43, p. 497. https://pubs.usgs.gov/tm/06/a43/.

Pérez-López, R., Carrero, S., Cruz-Hernández, P., Asta, M.P., Macías, F., Cánovas, C.R., Nieto, J.M., 2018. Sulfate reduction processes in salt marshes affected by phosphogypsum: geochemical influences on contaminant mobility. J. Hazard. Mater. 350, 154–161. https://doi.org/10.1016/j.jhazmat.2018.02.001.

Sáez, R., Pascual, E., Toscano, M., Almodóvar, G.R., 1999. The iberian type of volcano-sedimentary massive sulphide deposits. Miner. Depos. 34, 549–570. https://doi.org/10.1007/s001260050220.

Sarmiento, A.M., Nieto, J.M., Olías, M., Cánovas, C.R., 2009. Hydrochemical characteristics and seasonal influence on the pollution by acid mine drainage in the Odiel river basin (SW Spain). Appl. Geochem. 24, 697–714. https://doi.org/10.1016/j.apgeochem.2008.12.025.

Sherrell, R.M., Boyle, E.A., 1988. Zinc, chromium, vanadium, and iron in the Mediterranean Sea. Deep-Sea Res. 35, 1319–1334. https://doi.org/10.1016/0198-0149(88)90085-4.

Spivack, A.J., Huested, S.S., Boyle, E.A., 1983. Copper, nickel and cadmium in surface waters of the Mediterranean. In: Wong, C.S., Boyle, E., Bruland, K.W., Burton, J.D., Goldberg, E.D. (Eds.), Trace Metals in Seawater, 9. Springer, Boston, MA, pp. 505–512. https://doi.org/10.1007/978-1-4757-6864-0_30. NATO Conference Series.

Tamura, H., Goto, K., Yotsuyanagi, T., Nagayana, M., 1974. Spectrophotometric determination of iron(II) with 1,10-phenanthroline in the presence of large amounts of iron(III). Talanta 21, 314–318. https://doi.org/10.1016/0039-9140(74)80012-3.

Van Geen, A., Boyle, E.A., Moore, W., 1991. Trace metal enrichments in waters of the Gulf of Cadiz, Spain. Geochim. Cosmochim. Acta 55, 2173–2191. https://doi.org/10.1016/0016-7037(91)90095-M.

Van Geen, A., Adkins, J.F., Boyle, E.A., Nelson, C.H., Palanques, A., 1997. A 120 yr record of widespread contamination from mining of the Iberian Pyrite Belt. Geology 25, 291–294. https://doi.org/10.1130/0091-7613(1997)025<0291:AYROWC>2.3.CO;2.

Yu, J.Y., Heo, B., Choi, I.K., Cho, J.P., Chang, H.W., 1999. Apparent solubilities of schwertmannite and ferrihydrite in natural stream waters polluted by mine drainage. Geochim. Cosmochim. Acta 63, 3407–3416. https://doi.org/10.1016/S0016-7037(99)00261-6.

Zhou, J.L., Liu, Y.P., Abrahams, P.W., 2003. Trace metal behavior in the Conwy estuary, North Wales. Chemosphere 51, 429–440. https://doi.org/10.1016/S0045-6535(02)00853-6.